

Supporting Information for

“Cell Size as a Primary Determinant in Targeted Nanoparticle Uptake”

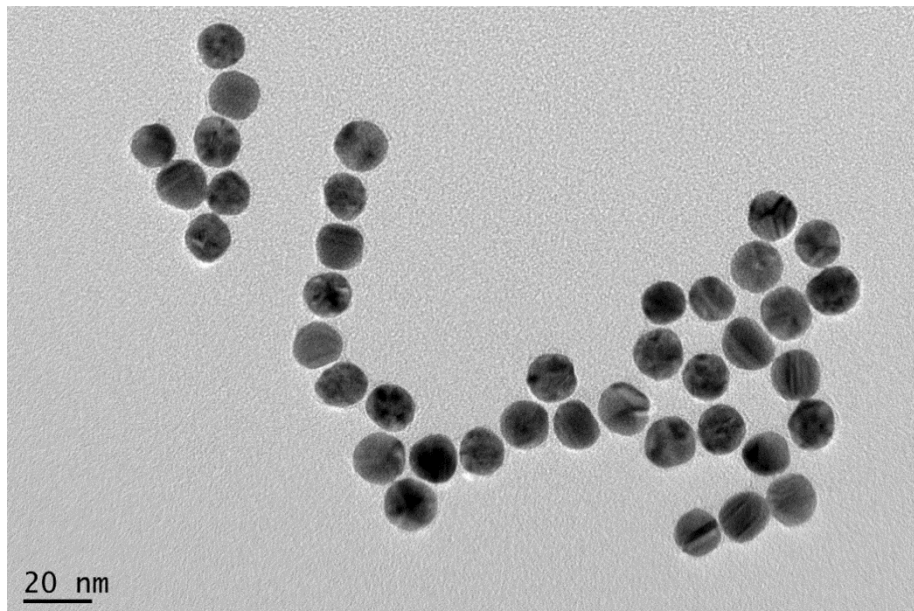
Douglas Howard¹, Tyron Turnbull¹, David J. Paterson², Benjamin Thierry¹, Ivan

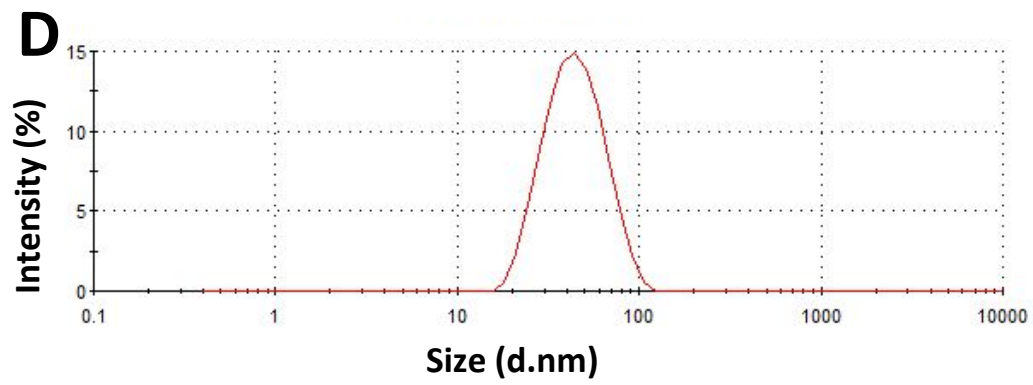
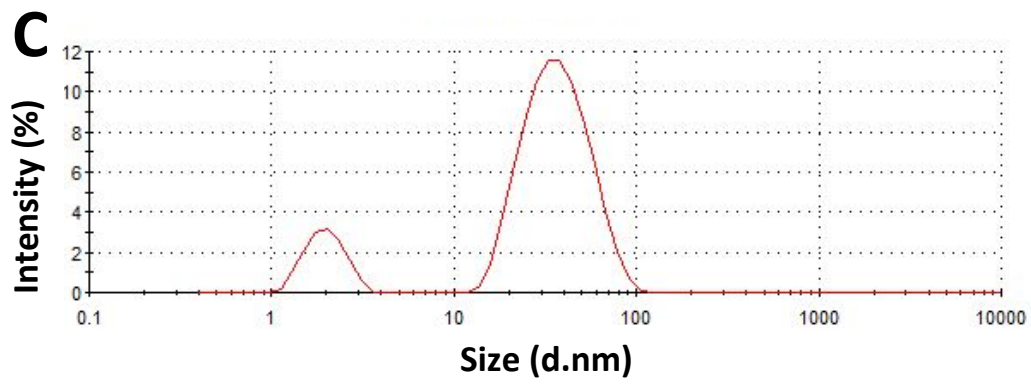
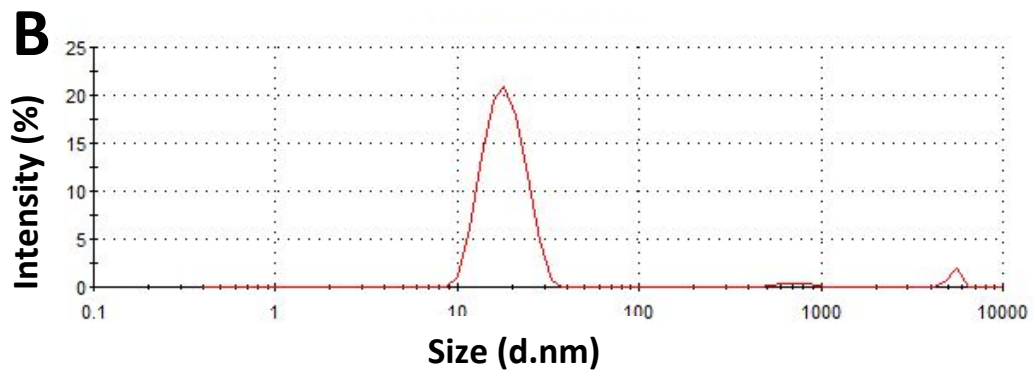
Kempson^{1*}

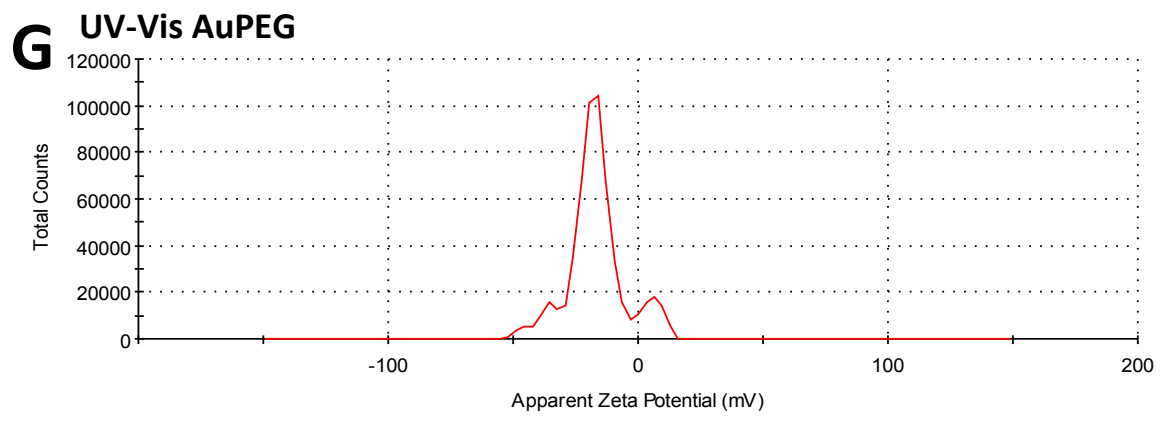
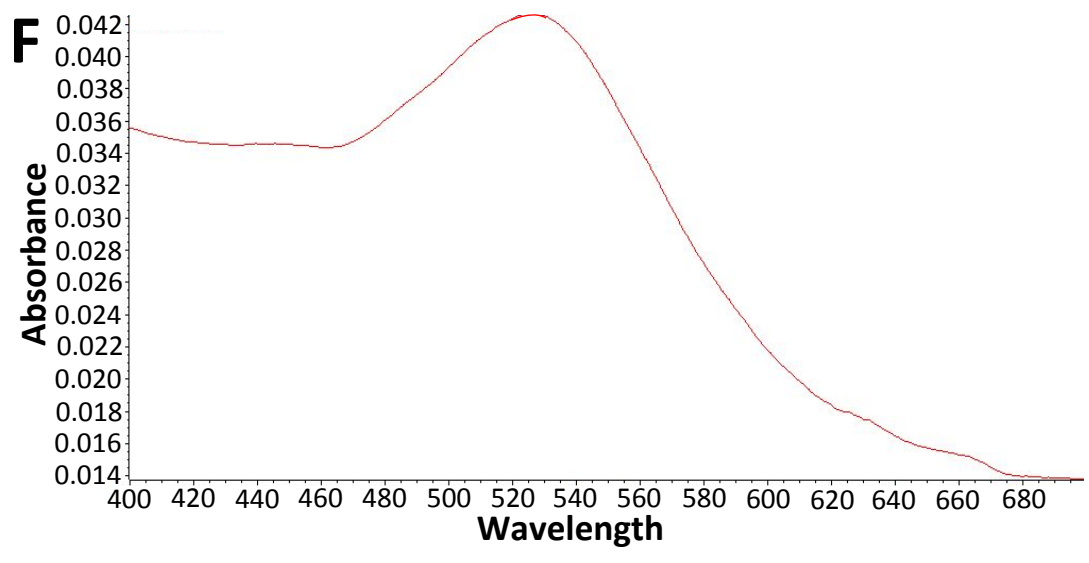
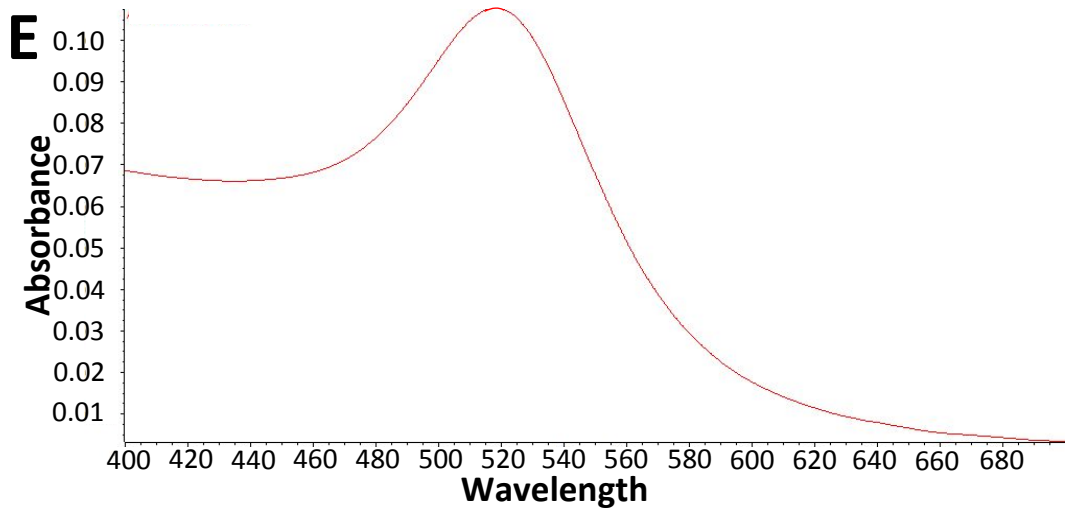
¹Future Industries Institute, University of South Australia, Mawson Lakes, SA 5095, Australia

²Australian Synchrotron, ANSTO, 800 Blackburn Road, Clayton, VIC 3168, Australia

A







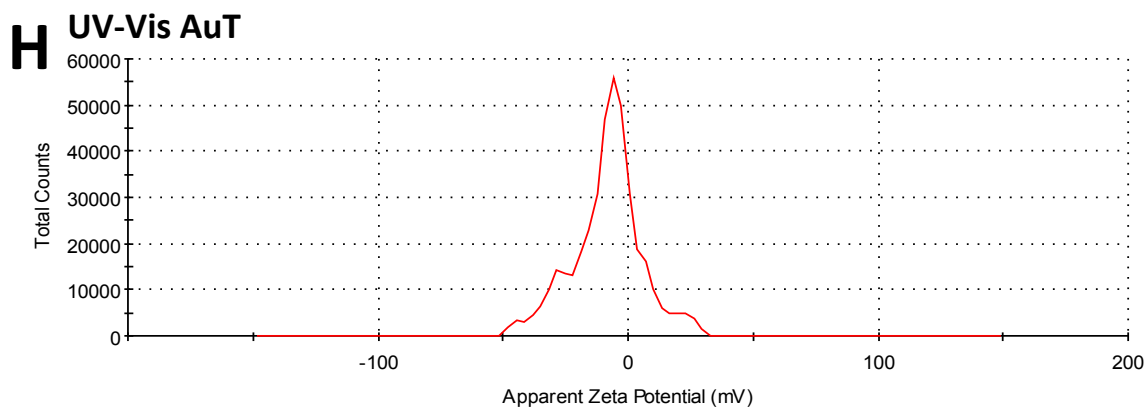


Figure S1. Characterization of the gold NPs. (A) Transmission

Technique	Au sol	AuPEG	AuT
DLS size (nm)	18.5	38.8	46.5
DLS zeta potential (mV)	-	~-6	~-12
UV-Vis peak (nm)	518.6	-	525.6

electron microscopy image of gold sol NPs on a copper grid. Dynamic light scattering (DLS) of the hydrodynamic size distribution by intensity for the gold sol (B), AuPEG (C) and AuT (D) NPs. UV-Vis spectroscopy was used to confirm successful conjugation of transferrin, demonstrated by the peak shift in the absorbance between Au sol (E) and AuT (F) NPs. Zeta potential plots are provided for the AuPEG (G) and AuT (H) NPs respectively.

Table S1. Dynamic light scattering hydrodynamic size peak and UV-Vis spectroscopy peak absorbance wavelengths for gold sol, AuPEG and AuT NPs.

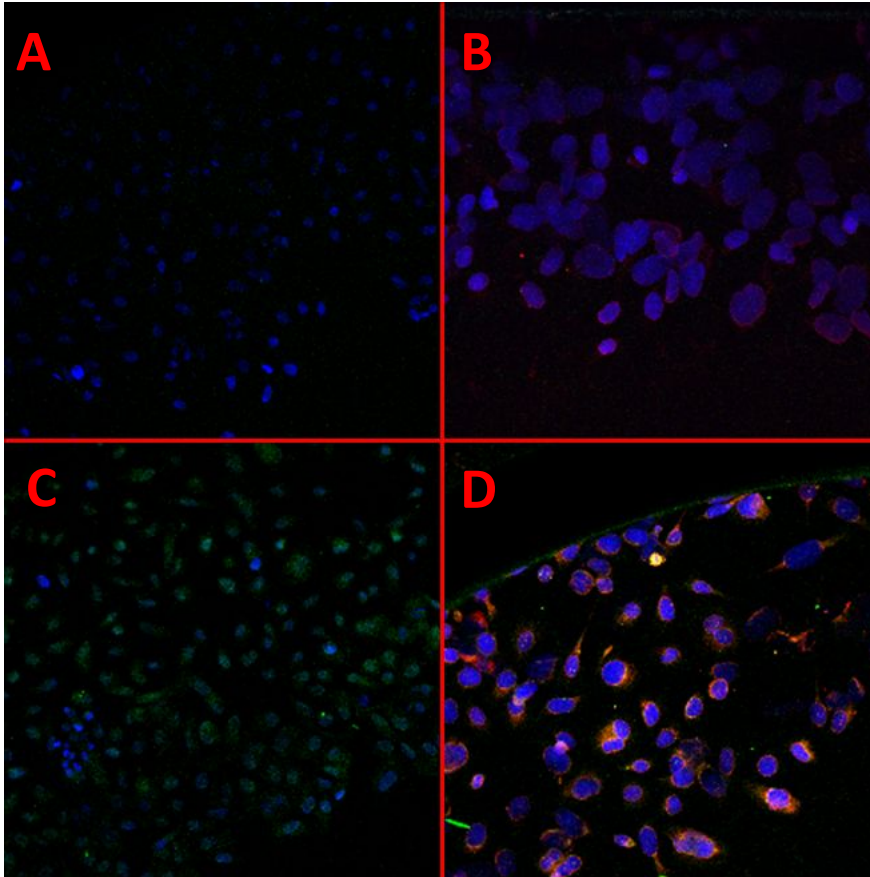
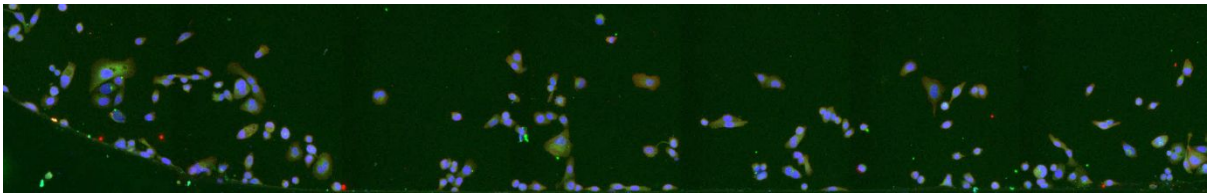
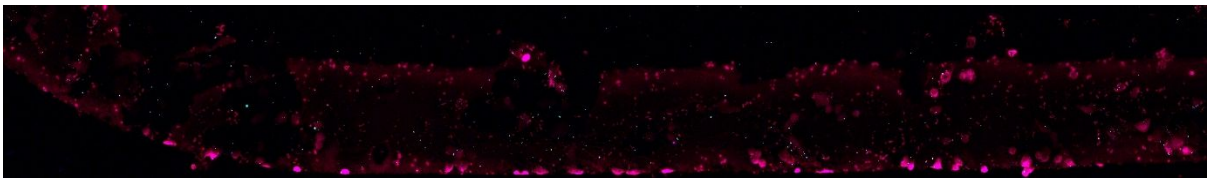
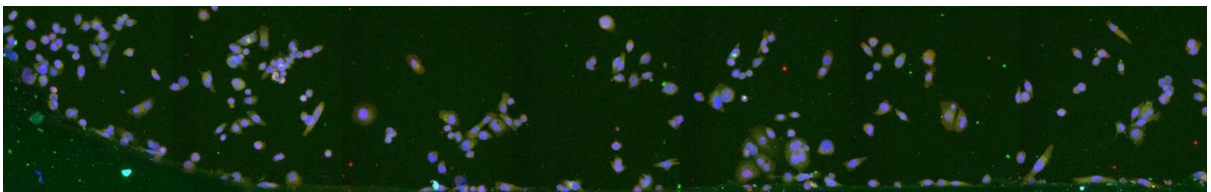
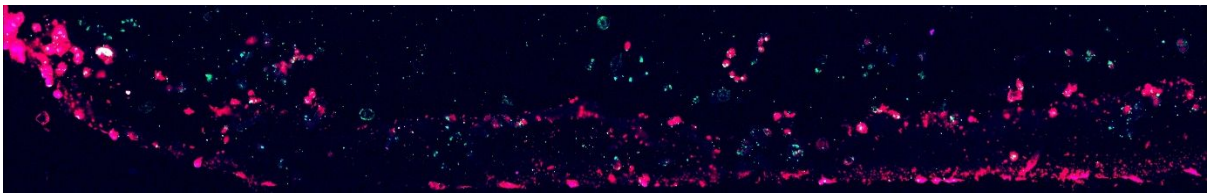


Figure S2. Confocal microscopy of fluorescent marker negative staining displaying; (A) DAPI staining, (B) DAPI and TfR2 staining, (C) DAPI and CD71 staining and (D) DAPI, CD71 and TfR2 staining. Each image was taken by analysing for all three channels.

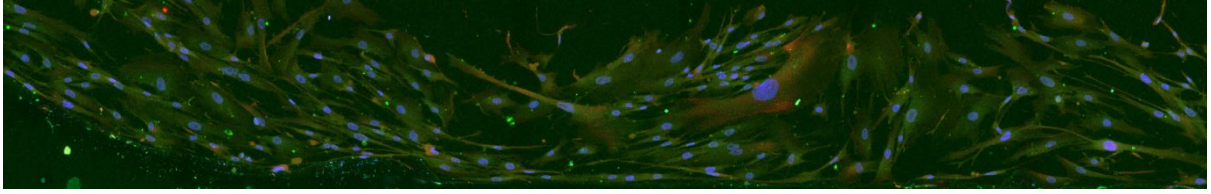
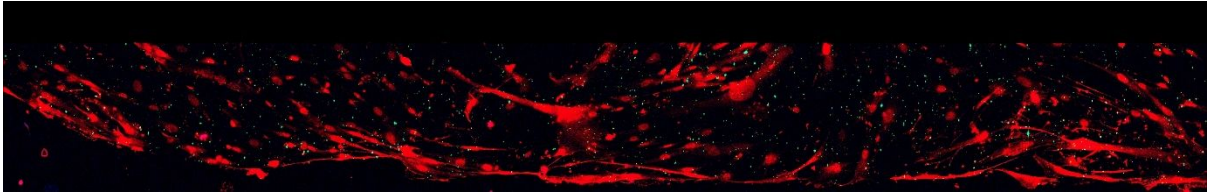
PC3 Au PEG



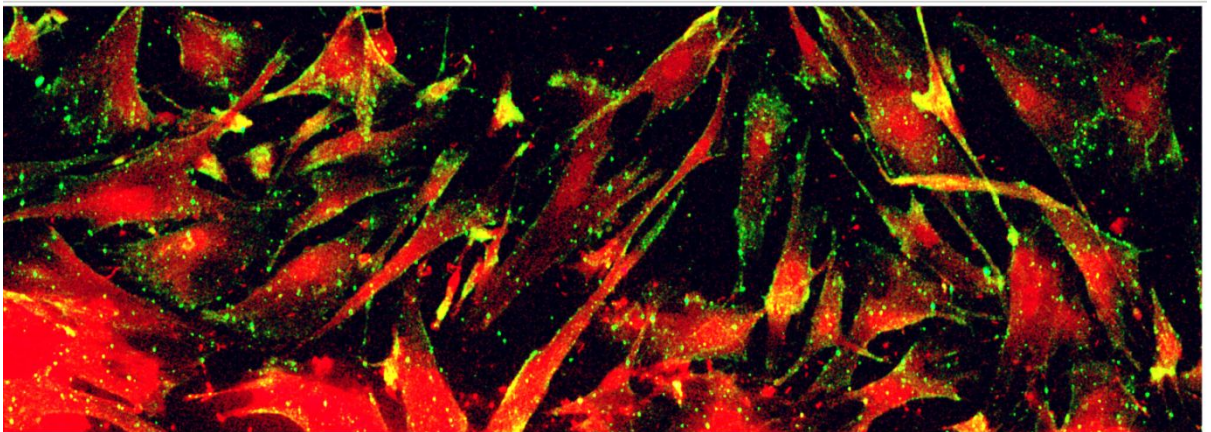
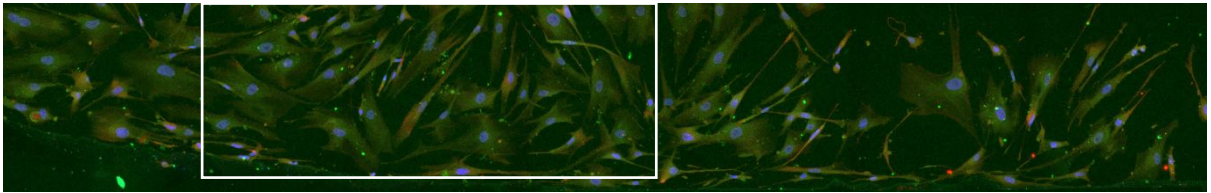
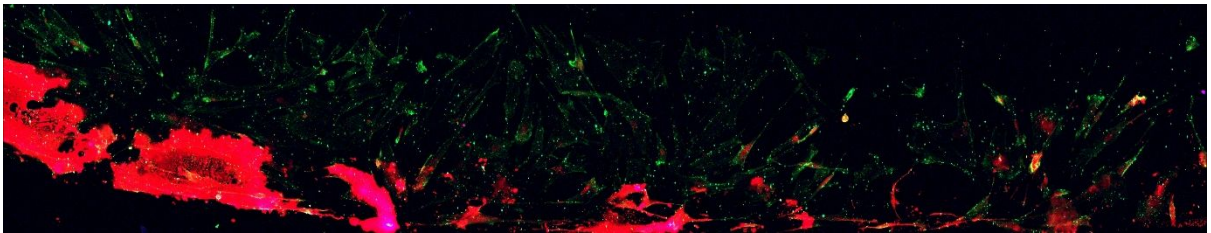
PC3 AuT



HFF Au PEG



HFF AuT



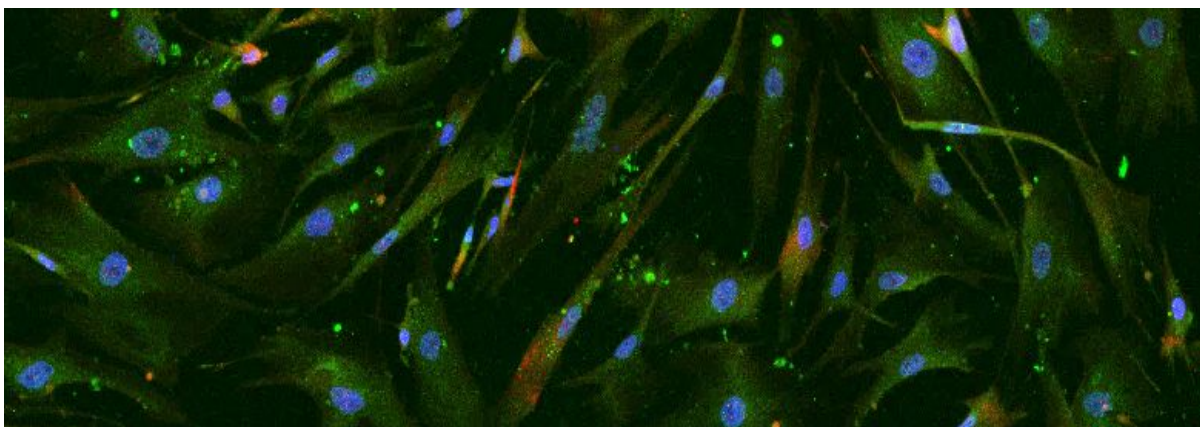


Figure S3. XRF and corresponding confocal microscopy images for each condition. XRF maps show copper and backscatter in pink/red and gold as green/cyan. Confocal maximum projection images show DAPI (blue), TfR2 (red) and CD71 (green). A zoomed-in image is included for the HFF AuT sample as indicated by the white box. Each cell region was identified from the CD71 channel manually in MATLAB.

The CD71 mask was overlaid onto the XRF gold map to identify subsequent cell regions on the gold elemental map. The pixel values were converted into their physical size in cm^2 to allow the integration process to yield a value in mass. Thresholds were included within the analysis process to identify and exclude apoptotic cells. Lognormal fitting of probability density functions was performed in MATLAB.

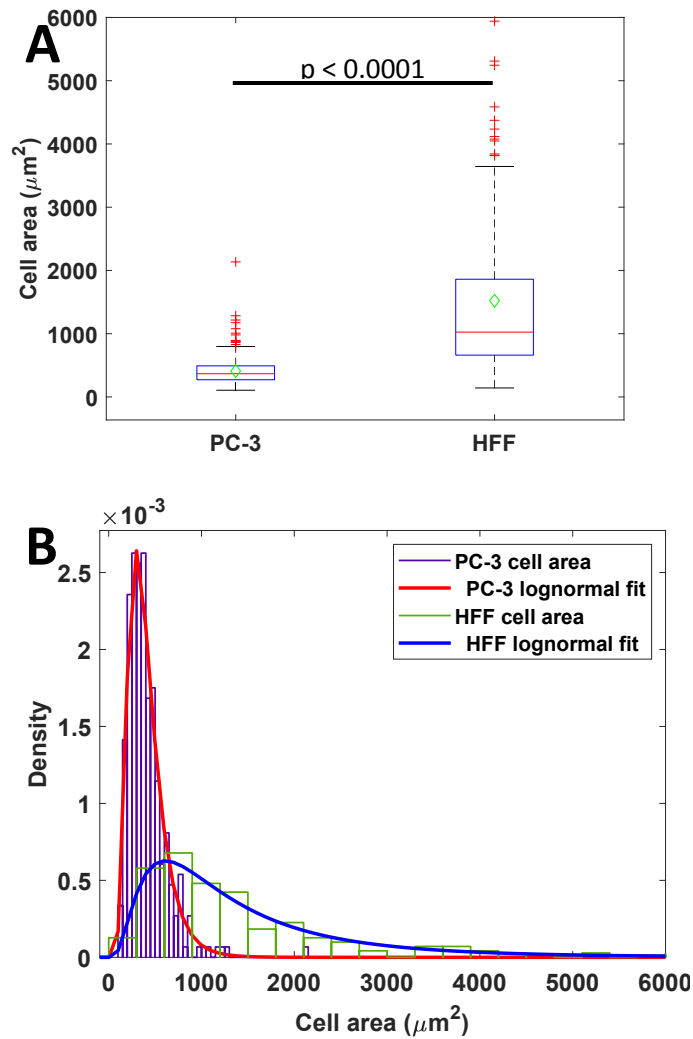


Figure S4. HFF cells are larger and more heterogenous than PC-3 cells. (A) Box and whisker plot of cell area for PC-3 and HFF cells. Boxes contain 25-75 percentiles of the data, separated by the red horizontal line representing the median. Whiskers represent the 0.7 and 99.3 percentiles; red 'plus signs' indicate outliers; green diamonds represent the mean. (B) Lognormal PDFs of the cell area for the PC-3 and HFF cell line populations.

Table S2. Evaluated statistics of the cell area in μm^2 with the mean, median and lognormal

PDF fitting parameters for the PC-3 and HFF cell lines.

	n	Mean (μm^2)	Median (μm^2)	μ	σ
PC-3	297	409	367	5.90	0.457
HFF	236	1521	1025	7.01	0.775

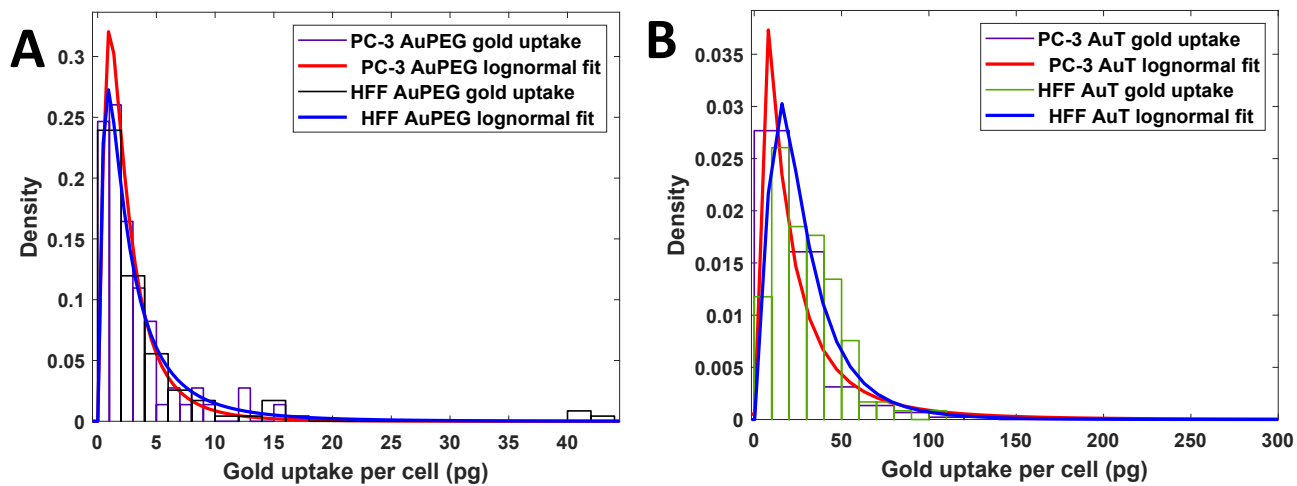


Figure S5. Probability density functions of AuPEG (A) and AuT (B) NP association in the PC-3 and HFF cell lines.

Table S3. Evaluated statistics of the AuPEG and AuT NP association with the lognormal PDF

fitting parameters for the PC-3 and HFF cell lines.

		n	μ	σ
PC-3	AuPEG	73	0.736	0.851
	AuT	221	2.79	1.07
HFF	AuPEG	117	0.878	1.02
	AuT	119	3.17	0.705

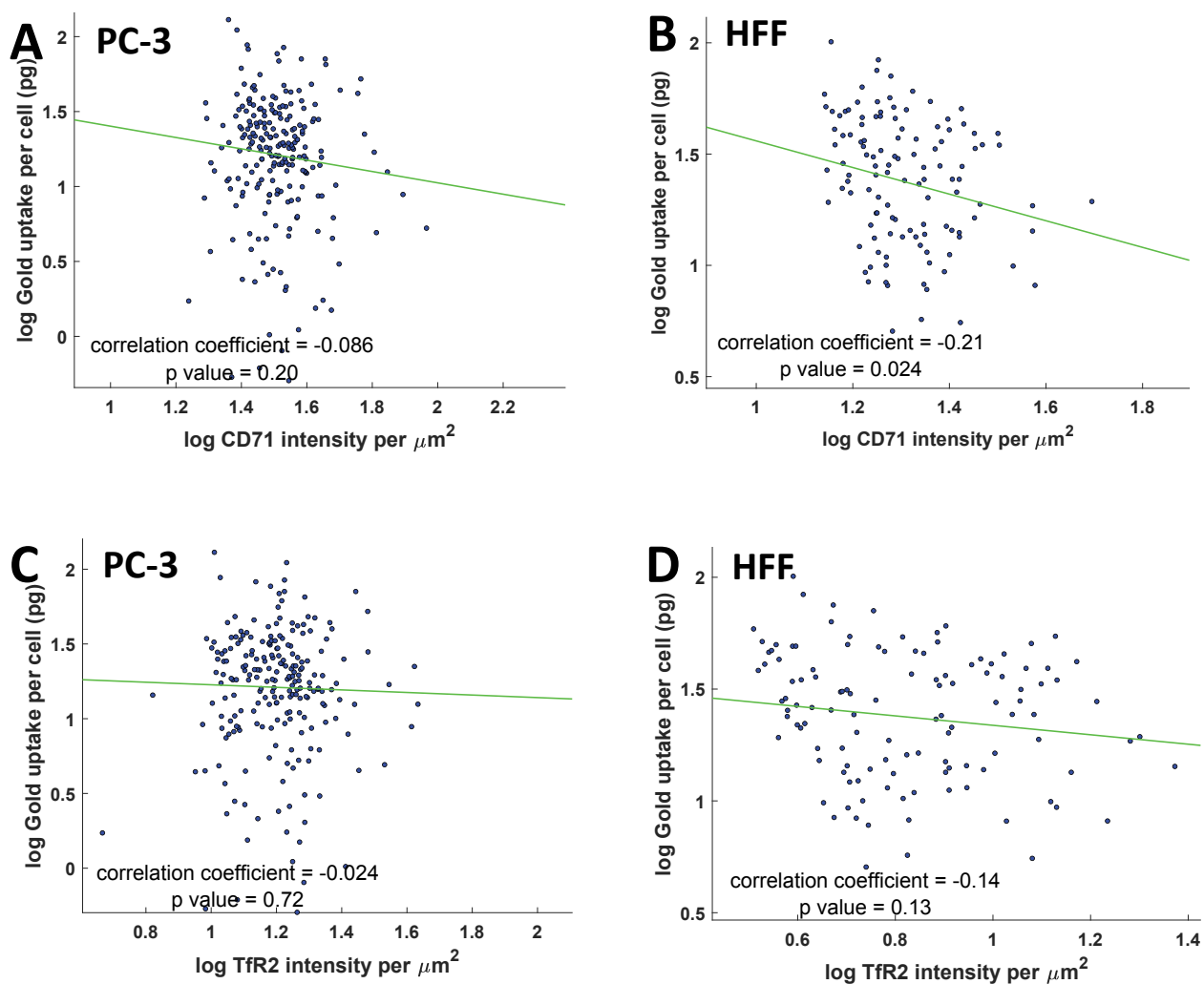


Figure S6. Targeted NP association is not correlated with receptor density. Scatterplots of CD71 (Tfr1) fluorescence intensity compared to the AuT NP association in the PC-3 cell line

(A) and the HFF cell line (B). The TfR2 fluorescence intensity for the AuT NP association in the PC-3 cell line (C) and the HFF cell line (D) is also presented. Note that data is presented on a log scale as both data sets are lognormally distributed, the log of the data was taken of each axis, and linear correlations were made.

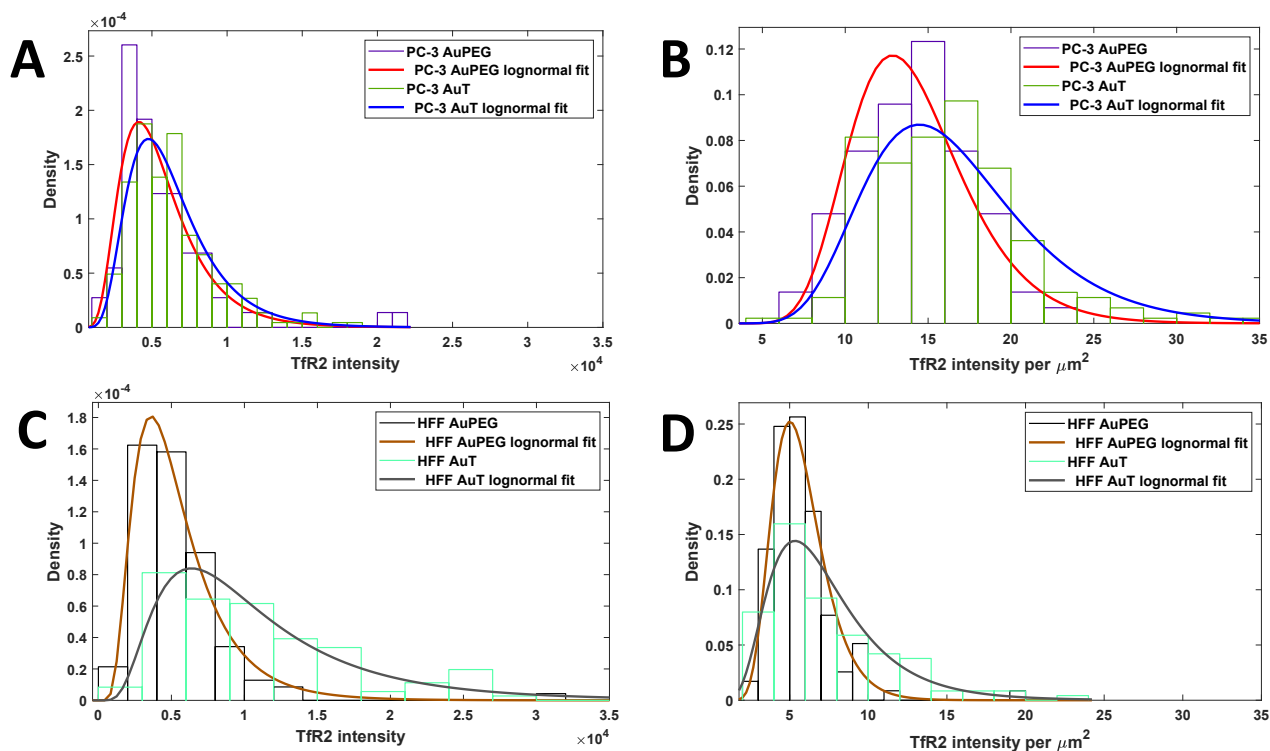


Figure S7. Probability density functions of Tfr2 fluorescence intensity of the PC-3 (A) and HFF (C) cell lines and Tfr2 density measured by Tfr2 fluorescence intensity per cell area in μm^2 for the PC-3 (B) and HFF (D) cell lines.

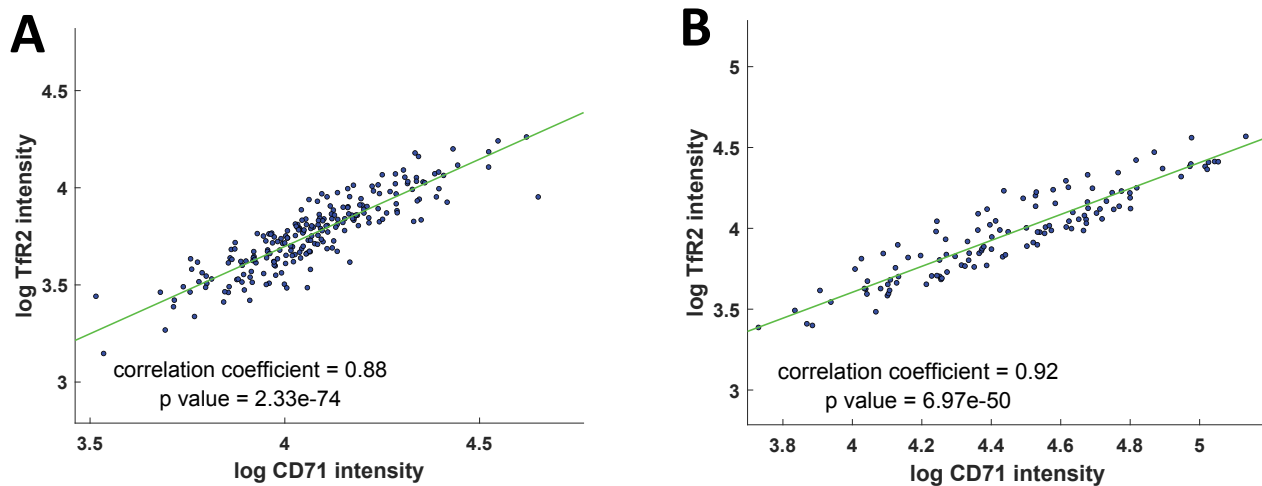


Figure S8. Scatterplot of the CD71 (TfR1) fluorescence intensity compared to the TfR2 fluorescence intensity for the AuT NP condition in the PC-3 cell line (A) and HFF cell line (B).

Note that data is presented on a log scale as both data sets are lognormally distributed, the log of the data was taken of each axis, and linear correlations were made.

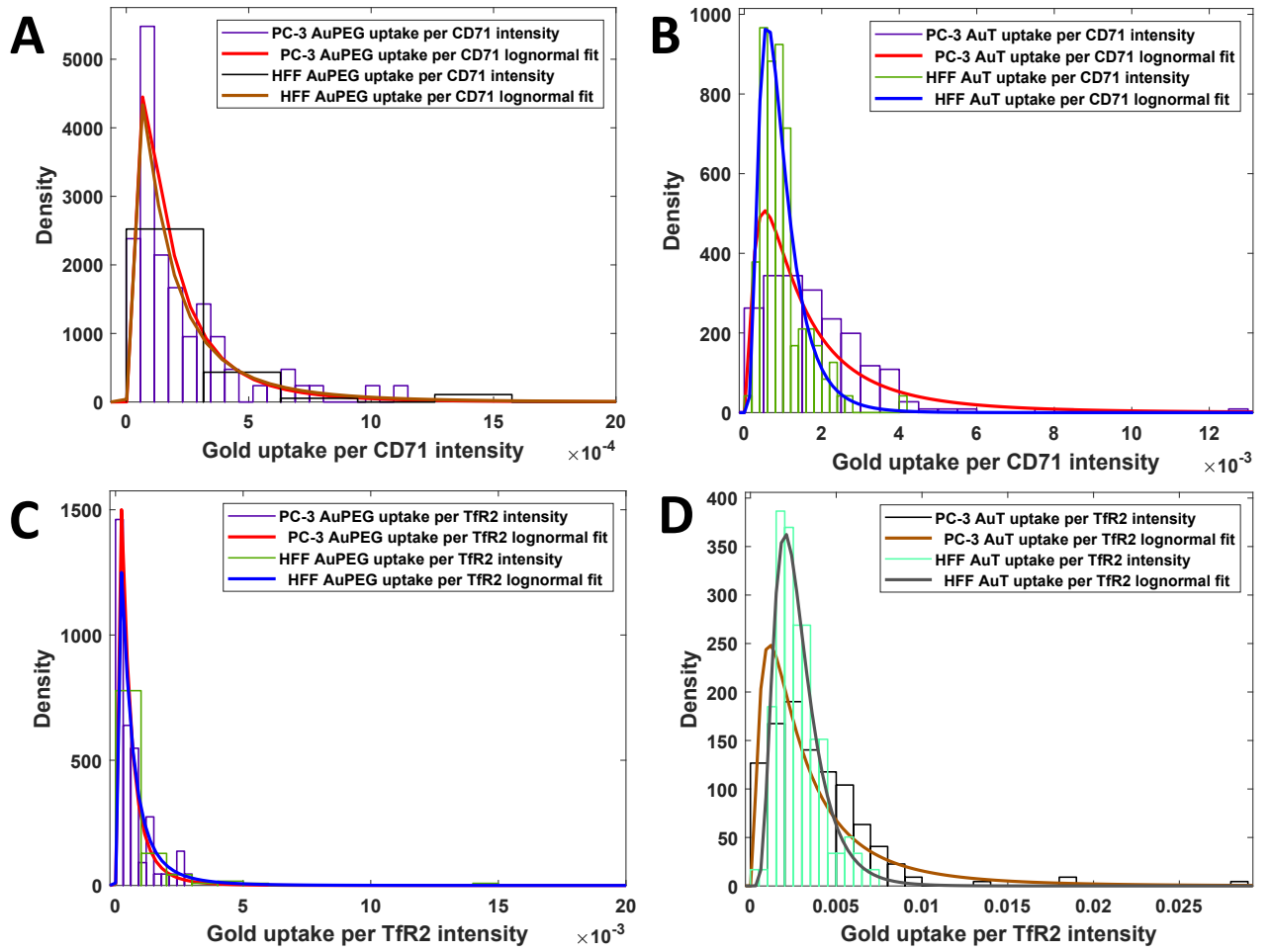


Figure S9. Probability density functions of AuPEG (A) and AuT (B) NP association per CD71 fluorescence intensity and AuPEG (C) and AuT (D) NP association per Tfr2 fluorescence intensity of the PC-3 and HFF cell lines.

Table S4. Evaluated statistics of the NP association correlated with CD71 and TfR2 receptor expression with the mean, median and lognormal PDF fitting parameters for the PC-3 and HFF cell lines.

	n	Condition	Mean (pg)	Median (pg)	μ	σ
PC-3	73	AuPEG per CD71 intensity	2.25e-4	1.42e-4	-8.81	0.906
		AuPEG per TfR2 intensity	6.47e-4	4.10e-4	-7.80	0.960
	221	AuT per CD71 intensity	0.003	0.002	-6.65	0.959
		AuT per TfR2 intensity	0.007	0.003	-5.93	0.936
HFF	117	AuPEG per CD71 intensity	2.94e-4	1.32e-4	-8.84	1.05
		AuPEG per TfR2 intensity	0.001	4.69e-4	-7.59	1.04
	119	AuT per CD71 intensity	9.77e-4	8.28e-4	-7.09	0.580
		AuT per TfR2 intensity	0.003	0.003	-5.97	0.484

Corresponding Author

Ivan Kempson – University of South Australia, Mawson Lakes, S.A., 5095, Australia.

<https://orcid.org/0000-0002-3886-9516> Email: Ivan.Kempson@unisa.edu.au